Send Orders for Reprints to reprints@benthamscience.net

Letters in Drug Design & Discovery, **2020**, *17*, 000-000

RESEARCH ARTICLE

Molecular Insights into the Interaction of Ursolic Acid and Cucurbitacin from Colocynth with Therapeutic Targets of *Mycobacterium tuberculosis*

M. Ajmal Ali[1,*], Mohammad Abul Farah[2,*], Joongku Lee[3], Khalid M. Al-Anazi[4] and Fahad M.A. Al-Hemaid[1]

[1]*Department of Botany and Microbiology, College of Science, King Saud University, Riyadh-11451, Saudi Arabia;* [2]*Department of Zoology, College of Science, King Saud University, Riyadh- 11451, Saudi Arabia;* [3]*Department of Environment and Forest Resources, Chungnam National University, 99 Daehak-ro, Yuseong-gu, Daejeon 34134, Republic of Korea*

ARTICLE HISTORY

Received: December 15, 2019
Revised: February 23, 2020
Accepted: April 06, 2020

DOI:
10.2174/1570180817999200514102750

Abstract: ***Aims*:** Medicinal plants like *Citrullus colocynthis* are a potential choice to produce helpful novel antimycobacterial drugs. The existence of a range of natural products in the plants, especially Ursolic Acid (UA) and cucurbitacin E 2-0-b-d-glucopyranoside (CEG), with promising antibacterial activity against a variety of bacteria, prompted the need to check its actions against *Mycobacterium tuberculosis* (Mtb).

***Background*:** *Mycobacterium tuberculosis* (Mtb), an obligate human pathogen causes tuberculosis and is one of the major causes of death worldwide. A few combinations of drugs are currently accessible for treating TB patients, but these are inadequate to tackle worldwide TB cases.

***Objective*:** The molecular interactions between ursolic acid and cucurbitacin E with the eight potential Mtb target proteins were investigated with the objective of finding drug-like inhibitors.

***Method*:** Avogadro v.1.2.0 and Openbabel v.2.4.1 were used for creating file formats required for docking analysis. Molecular docking was performed with eight different proteins essential for Mtb metabolism and survival. AutoDock v.4.2 and AutoDock vina v.1.1.2 were used for docking and Gromacs 5.1.4 was used for simulation studies.

***Results*:** Among the two ligands used in this research, cucurbitacin E showed a better docking score relative to the drugs presently available for all the target proteins. Rifampicin showed the best binding affinity (among known inhibitors) *i.e.* -10.8 kcal/mol with C terminal caspase recruitment domain. Moreover, ursolic acid and cucurbitacin E showed uniform binding score (above -7.5 kcal/mol) with all the target proteins, acknowledged its availability as a potential multi-target drug.

***Conclusions*:** Ursolic acid can be useful in the creation of novel, multi-targeted and effective anti-TB medicines since it showed stable structure with FabH.

Keywords: AutoDock, binding affinity, toxicity, hydrophobicity, ursolic acid, cucurbitacin E.

1. INTRODUCTION

Tuberculosis (TB) is a contagious infection caused by *Mycobacterium tuberculosis* (Mtb), s primarily affects the lungs. TB is an airborne disease that spreads through small droplets released into the air through coughs and sneezes from one individual to another [1]. Not all infected individuals acquire TB (latent tuberculosis); individuals infected with tuberculosis bacteria are 5% to 15% likely to fall ill [2]. It was the main cause of death in the early 20th century and is presently one of the top ten causes of death worldwide [3]. However, in recent times, antibiotics and various combinations of drugs are being developed to combat tuberculosis but require longer medication time to cure tuberculosis. In 2017, approximately 10 million people developed TB, and 1.6 million died because of TB. In developing countries, it possesses more threats because of its co-occurrence with several other diseases like HIV, malaria, *etc* [4]. In these scenarios, it becomes difficult to treat the diseased person. Recently, 0.3 million people died because of the lethal combination of TB and HIV (WHO report).

Mtb belongs to the Mycobacteriaceae family, first discovered by Robert Koch in 1882 [5]. Because of the exist-

*Address correspondence to these authors at the Department of Botany and Microbiology, College of Science, King Saud University, Riyadh-11451, Saudi Arabia; E-mail: ajmalpdrc@gmail.com and Department of Zoology, College of Science, King Saud University, Riyadh- 11451, Saudi Arabia; E-mail: mfarah@ksu.edu.sa

1570-1808/20 $65.00+.00

ence of a hydrophobic alpha-branched lipid, *i.e.* mycolic acid (gives waxy layer), it may appear as gram-positive or gram-negative [6]. Mtb requires oxygen for its metabolic processes. Over the year, different strains of Mtb are discovered; for example, multi-drug resistant TB (MDR-TB), extensively drug-resistant TB (XDR-TB) and totally drug-resistant TB (TDR-TB) [7]. Mtb strains develop resistance against drugs due to the accumulation of mutations in the antibiotic-targeted gene or due to the change in drug titration [8]. This let the emergency to develop new anti-TB drugs. A few combinations of drugs are currently accessible for treating TB patients, but these are inadequate to tackle worldwide TB issues. Despite the availability of these drugs, each year, the number of TB infected individuals increases along with drug-resistant strains of Mtb. Therefore, new TB drugs need to be developed for drug-sensitive and drug-resistant TB with shorter therapy time, being easier, more efficient (less toxic) but inexpensive. Development of a single drug with the efficiency to attack multiple targets, where, each target protein has some significant contribution to the development of a specific disease, is required. This will decrease toxicity and side effects relative to the TB drugs presently available. Progress in computational modelling and research of molecular interaction has opened the window for pre-laboratory molecular testing.

Mtb isocitrate lyase (MtbICL) is responsible for catalyzing the first step in the glyoxylate cycle and thus plays a pivotal role in the survival and persistence of Mtb [9]. Moreover, ICL is not present in humans; therefore, it can be used as a potential candidate for the design of TB drugs. ICL catalyzes the cleavage of isocitrate to glyoxylate and succinate. The conformational change triggered by ligand binding to the active site results in deprotonation of isocitrate and subsequent aldol condensation causes succinate and glyoxylate release from the active site. Besides ICL, several enzymes engaged in essential physiological activities in Mtb were recognized as novel attractive molecular targets for anti-TB drug development. Decaprenyl phosphoryl- β -D-ribose 2 epimerase 1 (DprE1) catalyzes FAD-dependent oxidation of the C2' hydroxyl of DPR to yield the keto intermediate decaprenyl-phospho-2'-keto-D-arabinose (DPX) [10]. Mycobacterial enzyme beta-ketoacyl-acyl carrier protein synthase III plays a key role in the synthesis of mycolic acids [11]. Following this, another enzyme, namely *dTDP-6-deoxy-D-xylo-4-hexulose 3, 5-epimerase* (RmIC) is crucial for cell wall biosynthesis in Mtb. Mycobactin synthase (MS) produces mycobactin, which is vital when it is in an infected host for the bacterium to access iron [12]. N-acetylglucosamine-6-phosphate deacetylase (NagA) plays a part in the generation of vital amino-sugar precursors needed for Mtb cell wall biosynthesis [13]. ATP-synthase rotor ring, as the name suggests, is a key metabolic enzyme required for ATP generation. C-terminal caspase recruitment domain (CarD) interacts with the β-subunit of RNAP and this interaction is vital for Mtb survival during the persistent infection state [14]. Therefore, *in-silico* screening of these key enzymes against naturally occurring plant secondary metabolites could provide a significant clue about the possibility of their usage as drug targets and potential inhibitory ligands, respectively.

Plants are the natural sources of biologically active secondary metabolites having an enormous role in therapeutics [15]. Medicinal plants like *Citrullus colocynthis* are a potential choice to produce effective novel antimycobacterial drugs. Studies have been carried out revealing the chemical constituents and medicinal use of various compounds produced by *C. colocynthis*; a perennial desert plant abundantly found in the sandy arid regions of Africa, Mediterranean and Indo-Malaysian regions [16]. The existence of a range of natural products in the plants, especially ursolic acid (UA) and cucurbitacin E 2-0-β-d-glucopyranoside (CEG), with promising antibacterial activity against a variety of bacteria, prompted the need to check their actions against MTB and several other human diseases [17]. UA is a secondary plant metabolite that has been found to possess a wide range of therapeutic properties ranging from antibacterial, antiviral, anticancer, antioxidant to antimycotic activity [18]. Moreover, this phytocompound significantly inhibited the growth of both sensitive and drug-resistant forms of tubercle bacilli *in vitro*, proving strong anti-mycobacterial properties [19]. Anti-mycobacterial properties of ursolic acid have been demonstrated to activate the intracellular killing cascades of hosts during mycobacterial infection [20,21]. While , UA and CEG from *C. colocynthis* were identified as the main biomarkers active against *Mycobacterium tuberculosis* [22]. To treat bacterial infections and respiratory diseases, indigenous people use *Cucurbitaceae* as a natural remedy. *Cucurbitaceae* has many other important metabolites that are used for various medicinal purposes. Researchers have recently been searching for natural biologically active substances that have the ability to be used as drugs [23]. This leads researchers to return to the ancient understanding that has been obtained over generations. So far, ursolic acid and cucurbitacin E 2-0-β-d-glucopyranoside have not been reported in detail against Mtb. Here we docked these two ligands (using AutoDock vina and autodock) against the eight vital enzymes of mycobacterium to validate their use as a prospective Mtb drug.

2. MATERIALS AND METHODS

2.1. Data Collection

The crystal structure information of eight essential mycobacterial enzymes was retrieved from RCSB PDB (www.rcsb.org) database. Based on the literature survey, the following target enzymes were selected for the present study: isocitrate lyase (ICL) (PDBID: 1F8I) [24], decaprenyl phosphoryl-B-D-ribose 2 epimerase 1 (DprE1) (PDBID: 6HFV) [25], beta-ketoacyl-acyl carrier protein synthase III (FabH) (PDBID: 1HZP) [26], mycobactin synthase (MS) (PDBID: 2G5F) [12], dTDP-6-deoxy-D-xylo-4-hexulose 3,5 epimerase (RmIC epimerase) (PDBID: 1UPI) [27], N-acetylglucosamine-6-phosphate deacetylase (NagA) (PDBID: 6FV3) [28], ATP synthase rotor ring (ASRR) (PDBID: 4V1H) [29] and C-terminal caspase recruitment domain (CARD) (PDBID: 4KBM) [30]. Next, the two ligands structure *i.e.* ursolic acid (L1)(ZINC03978827) and cucurbitacin E 2-O-β-D-glucopyranoside (L2) (ZINC040978000) was retrieved from ZINC database (https://zinc.docking.org/).

Table 1. List of known inhibitors used with database ID and smiles.

S. No.	Ligands	Database ID
1	Ursolic acid (L1)	PubChem CID:64945; ZINC03978827
2	Cucurbitacin E 2-0-b-d-glucopyranoside (L2)	CHEBI:68916; ZINC040978000
3	Isoniazid (KI-1)	PubChem CID:3767; ZINC00001590
4	Rifampicin (KI-2)	PubChem CID:135398735; ZINC94313219
5	Pyrazinamide (KI-3)	PubChem CID:1046; ZINC00002005
6	Streptomycin (KI-4)	PubChem CID:19649; ZINC08143632
7	Ethambutol (KI-5)	PubChem CID:14052; ZINC19364219
8	Ethionamide (KI-6)	PubChem CID:2761171; ZINC03872520
9	Kanamycin (KI-7)	PubChem CID:6032; ZINC08101133
10	Cycloserine (KI-8)	PubChem CID:6234; ZINC34676244
11	Thioacetazone (KI-9)	PubChem CID:9568512; ZINC17970372
12	P-aminosalicyclic (KI-10)	PubChem CID:342588352; ZINC00000922
13	Ofloxacin (KI-11)	PubChem CID:4583; ZINC00537891
14	Bedaquiline (KI-12)	PubChem CID:5388906; ZINC04655029
15	Sprafloxacin (KI-13)	ZINC00538362

2.2. Library Preparation and Toxicity Screening

Library preparation was done based on database and literature survey. For each of the target proteins, their corresponding known inhibitors data was retrieved from the ZINC database (https://zinc.docking.org/) and CHEBI database (https://www.ebi.ac.uk/chebi/). The list of potential inhibitors of Mtb proteins is given in Table **1**. Combinatorial libraries of about 200 derivatives were generated by adding the hydroxyl and pharm group to these known inhibitors (KI). Following this, drug likeliness of the compounds was assessed by using mobyle@rpbs server (http://mobyle.rpbs.univ-paris-diderot.fr/cgi-bin/portal.py). ADMET (Absorption, Distribution, Metabolism, Excretion, and Toxicity) screening helps in detecting drug likeliness of compounds. Following this, we used another tool *i.e.* ProTox-II (http://tox.charite.de/protox_II/) to validate the toxicity results of ligands [31]. All the compounds not passing the toxicity screening were discarded and all the drug-likeness compounds were subjected to docking with the target proteins.

2.3. Molecular Docking and Simulation

Avogadro v.1.2.0 and Openbabel v.2.4.1 were used to convert the file formats required for docking analysis [32, 33]. All the cofactors, waters and ligands were removed from the target proteins PDB file. We performed docking for all the ligands against all the receptors. Eight receptor proteins were docked against all the ligands passing the toxicity screening. We used AutoDock vina v.1.1.2 to dock the ligands against the potential receptors [34]. Furthermore, AutoDock v.4.2 [35] was used to compare the results of AutoDock Vina. The three-dimensional grid box was created by the AutoGrid algorithm to evaluate the binding energies on the macromolecule coordinates. Auto Dock was used for calculating the binding free energy of a given ligand conformation in the macromolecular structure, while the probable structure inaccuracies were ignored in the calculations. Grid box parameters were set in such a way so as to allow for a suitably-sized cavity space large enough to accommodate each compound within the binding site of each protein. The Lamarckian Genetic Algorithm was used during the docking process to explore the best conformational space for each ligand. The MD simulations using default protocols and parameters of the software GROMACS 4.6.5 [36] have been applied similar to the protocol followed elsewhere in our previous study [37].

2.4. Molecular Interactions Visualization

All the ligand and proteins docking results were visualized in python-enhanced molecular graphics tool UCSF Chimera (https://www.cgl.ucsf.edu/chimera/). Molecular interactions in the form of hydrogen bonds between target proteins and ligands were characterized and the distance of hydrogen bond was also calculated.

3. RESULTS

3.1. Toxicity and Molecular Docking Studies

In the field of structure-based drug designing, molecular docking plays the central role by screening smaller molecules for their binding potential to target proteins. Accordingly, novel ligands are discovered and it is estimated that

Table 2. Descriptors of ligand 1 (L1), ligand 2 (L2) and all known inhibitors (drugs).

Ligands	LD50 (mg/kg)	TC	MW (g/ml)	NHA	NHD	NA	NB	NR	NRB	TC	MPSC	logP
L1	2000	4	456.7	3	3	39	43	5	1	0	57.53	7.09
L2	3000	5	461.92	6	8	31	33	3	9	0	90.52	4.19
KI-1	133	3	137.14	4	14	10	10	1	2	0	68.01	3.00
KI-2	500	4	822.94	15	15	67	71	5	5	0	220.15	-7.742
KI-3	1800	4	123.11	4	15	9	9	1	1	0	69.86	-7.29
KI-4	224	3	581.57	19	6	54	56	3	11	0	333.43	1.20
KI-5	998	4	204.31	4	6	16	15	0	9	0	64.52	2.11
KI-6	1000	4	166.24	2	2	11	11	1	2	0	71	0.62
KI-7	10	2	484.5	15	4	48	50	3	6	0	282.61	7.02
KI-8	2492	5	102.09	4	1	7	7	1	0	0	64.35	1.28
KI-9	450	4	236.29	5	3	16	16	1	5	0	111.6	-0.31
KI-10	4000	5	153.14	4	3	11	11	1	1	0	83.55	0.68
KI-11	1478	4	361.37	6	4	27	30	4	2	0	75.01	-0.29
KI-12	1000	4	555.5	4	4	38	42	5	8	0	45.59	0.36
KI-13	2000	4	392.4	7	4	30	33	4	3	0	100.59	-1.17

*LD50: Lethal dose 50; TC: Toxicity class; MW: Molecular weight; NHA: No. Of Hydrogen bond acceptor; NHD: No. Of Hydrogen bond donor; NA: No. Of atoms; NB: No. Of bonds; NRB: No. Of rotable bonds; TC: Total charge; MPSC: Molecular polar surface area.

Table 3. Comparison of docking score of 2 ligands and 13 known inhibitors against the eight potential target proteins.

Sl. No.	Known Inhibitors	FabH	RmIC	NagA	DprE1	ICL	ASRR	MS	CARD
1	L1	-9.4	-9.0	-8.4	-9.5	-8.4	-7.5	-9.2	-10.1
2	L2	-9.4	-9.4	-9.3	-9.5	-9.7	-7.8	-10.6	-10.8
3	KI-1	-9.0	-8.6	-9.5	-8.6	-8.8	-7.1	-8.7	-10.8
4	KI-2	-8.3	-8.0	-7.8	-7.3	-7.4	-5.3	-6.8	-8.6
5	KI-3	-7.9	-7.5	-8.3	-8.0	-7.3	-6.1	-8.0	-8.2
6	KI-4	-7.8	-8.5	-8.1	-8.6	-7.2	-6.4	-9.2	-7.6
7	KI-5	-7.7	-8.0	-7.7	-8.4	-6.9	-6.0	-9.1	-8.0
8	KI-6	-6.8	-6.1	-6.9	-7.5	-6.0	-5.7	-6.3	-6.0
9	KI-7	-6.7	-6.8	-5.6	-8.2	-7.1	-5.6	-8.6	-7.2
10	KI-8	-5.6	-5.1	-5.2	-5.7	-5.2	-4.9	-5.5	-4.9
11	KI-9	-5.5	-4.9	-5.2	-5.9	-4.7	-4.8	-5.4	-5.4
12	KI-10	-5.2	-5.3	-5.7	-6.2	-6.6	-5.1	-5.4	-6.0
13	KI-11	-4.9	-4.3	-5.3	-5.2	-4.0	-3.8	-4.6	-4.3
14	KI-12	-4.3	-4.5	-5.2	-5.2	-5.8	-4.1	-4.9	-4.6
15	KI-13	-3.7	-4.1	-4.4	-4.7	-5.5	-3.3	-4.9	-4.5

*KI: Known Inhibitor; L: Ligand.

the docking programs correctly dock 75-85% of ligands. Based on the literature, some of the known inhibitors (KI) were used as controls to compare and validate the docking of our two ligands against the eight potential target proteins [38-41]. The drug likeliness properties of all the ligands used in the present study are shown in Table **2**. All the known inhibitors were re-docked to their respective target proteins using AutoDock and AutoDoct Vina. The docking score of each known inhibitors with their respective ligands was recorded (Table **3**). To measure the efficiency of a ligand to other potential target proteins, we docked each ligand against all the eight proteins. Similarly, our L1 and L2 were also docked against the eight target proteins. Both the ligands (L1 and L2) were found to inhibit the target proteins by showing a better binding affinity score. Among the KI, rifampicin showed the best docking with most of the target proteins. Rifampicin showed the docking score of -8.8 kcal/mol with ICL; -8.6 kcal/mol with DprE1; -9.0 kcal/mol with FabH; -8.6 kcal/mol with RmIC; -9.5 kcal/mol with NagA; -7.1 kcal/mol with ASRR; -10.8 kcal/mol with CARD. Out of all the KI, ofloxacin showed better docking than rifampicin for the protein MS. The docking score is -9.2 kcal/mol. Next, L1 and L2 were docked with all the proteins and their corresponding docking score was compared with KI. Surprisingly, except for the protein NagA, all other protein showed the best docking score with our ligands. When compared with each other, L2 showed a better score than L1. L1 showed the best docking with CARD, followed by DprE1, FabH, MS, RmIC. L1 showed the same docking score *i.e.* -8.4 kcal/mol with NagA and ICL. ASRR showed the lowest score with L1. Moreover, L1 revealed a better score than rifampicin for FabH, DprE1, ASRR and MS. Similar to L1, ASRR showed the lowest score with L2. CARD showed the best docking score (-10.8 kcal/mol) with L2, followed by MS, DprE1. L2 showed the same docking score *i.e.* -9.4 kcal/mol with FabH and RmIC. When compared with best KI *i.e.* rifampicin, L2 showed the best docking with all the target proteins except for NagA. NagA showed better docking with rifampicin than L2 and L1.

Specific interactions were further explored to understand the nature of the intermolecular bonds formed between L1 and eight target proteins, in the same way, L2 and eight target proteins. The binding interaction between the residues of protein and ligand was visually inspected for each of the docked structure. Fig. **1(a-c)** depicts the molecular docking as well as intermolecular interaction between FabH and L1. We observed that L1 showed some key hydrophobic interactions with the key residues, namely, Gln79, Gln80, Ala353; whereas hydrogen bond formation via Gln80 of ICL. L2 showed key hydrophobic interaction with the residue Leu69, Asn75, Gln80 and Ala 349,353,390, whereas hydrogen bond formation with Gln79 residue of ICL. DprE1 residue number Trp230, Asp232, Tyr297, and Pro316 showed hydrophobic interaction with L1, whereas, Trp230, Tyr297, Pro316, Phe362, and Leu363 confirmed with L2. L1 showed salt bridge formation with DprE1 via Arg242 residue. MS also showed crucial intermolecular hydrophobic interaction via the residue Glu43, Val60, Met63 and Ile74 with L1, similarly via Asp97, Leu100, Pro345 with L2. Glu39 and Ser40 residue of MS showed hydrogen bond formation with L1 and via Arg349 with L2. RmIC residue Glu143 showed hydrophobic interaction, where, Sre168 showed hydrogen bond formation with L1. L2 showed hydrophobic interaction with Leu25, Phe27, Trp29 and Val45-48 residues of RmIC, but showed hydrogen bond formation via Trp29, Leu30, and Val77. For NagA, Asn212, Ala213, and Ile301 showed their involvement in hydrophobic interaction whereas, Ala213 in hydrogen bond formation with L1. L2 shows both hydrophobic (Ala67, Tyr279, Arg280) as well as hydrogen bond formation (Arg102, Gln103) with NagA. ASRR showed less intermolecular interactions viz. hydrophobic (Leu53, Phe57 with L1; Val64, Ala67 with L2) and hydrogen bonds (via Thr60 with L1; Gly24, Gly27, and Asn71 with L2). CARD protein showed more hydrogen bonds with L2 than L1. Val50, Asp53, and Trp57 are involved in hydrophobic interaction, whereas Asp53 in hydrogen bond formation with L1. Val64, Ala67 residue is involved in hydrophobic interaction but Gly24, Gly27, and Asn71 in hydrogen bond formation with L2.

3.2. Identification of the Interaction Between FabH and L1

We analyzed the binding pattern between L1 and FabH. The trajectories were stable during the whole production part of 10 ns MD simulation run (Fig. **2**). The trajectory stability was monitored and was confirmed by the analysis of the potential energy as a function of time for the Mtb-FabH (Fig. **3**). The average short-range Coulmb interaction energy, short-range Lennard-Jones interaction energy and potential interaction energy between L1 and FabH were -5.75505, -142.467 and -2.32127e+06 kJ/mol. As anticipated, L1 stably docked to the Ligand-Binding Domain (LBD). The binding mode of L1 in the LBD of FabH provided detailed structural insight into the interaction between this compound and the FabH protein. Furthermore, we performed a 10-ns MD process using GROMACS 5.1.4 software. The time-averaged normalized ratio of the gyration radius, the RMSD, hydrogen bonds and the solvent-accessible surface area were analyzed to reflect the distribution of L1 molecules surrounding FabH (Fig. 4). RMSD measures the accuracy that is on average 0.4454 ± 0.2231. The RMSD values are stable up to 4 ns (0.2063741 ± 0.0355 nm) of simulation for Mtb-FabH in Fig. **4(a)** and then increases in the following simulation time. A rise in the value after 4 ns is attributable to the relaxation motion of the protein or inaccuracy in the force field. The gyration radius of the ligand L1 and the receptor FabH represents the compactness of and stability in the protein with an average value of 1.967179 ± 2.097486e-02 nm that trended toward stability as time progressed (Fig. **4b**). Furthermore, Solvent Accessible Surface area (SASA) (Fig. **4c**) analysis of protein measures the proportion of the biomolecules' surface interacting with the water solvent, which also represented a stable surface area of the protein with an average value 151.5282 ± 2.391937 nm. The calculation of SASA can be used for predicting the extent of the conformational changes occurring during the course of binding. L1 potentially formed hydrogen bonds with ARG151 and ASN247. The interacting H-bond number was found to change in a stable range (Fig. **4d**). A total of 2-4 hydrogen bonds were formed between the protein-ligand complexes during production MD, showing the stability of ligand binding. From the whole MD simulation, it can be ascertained that the ligand showed

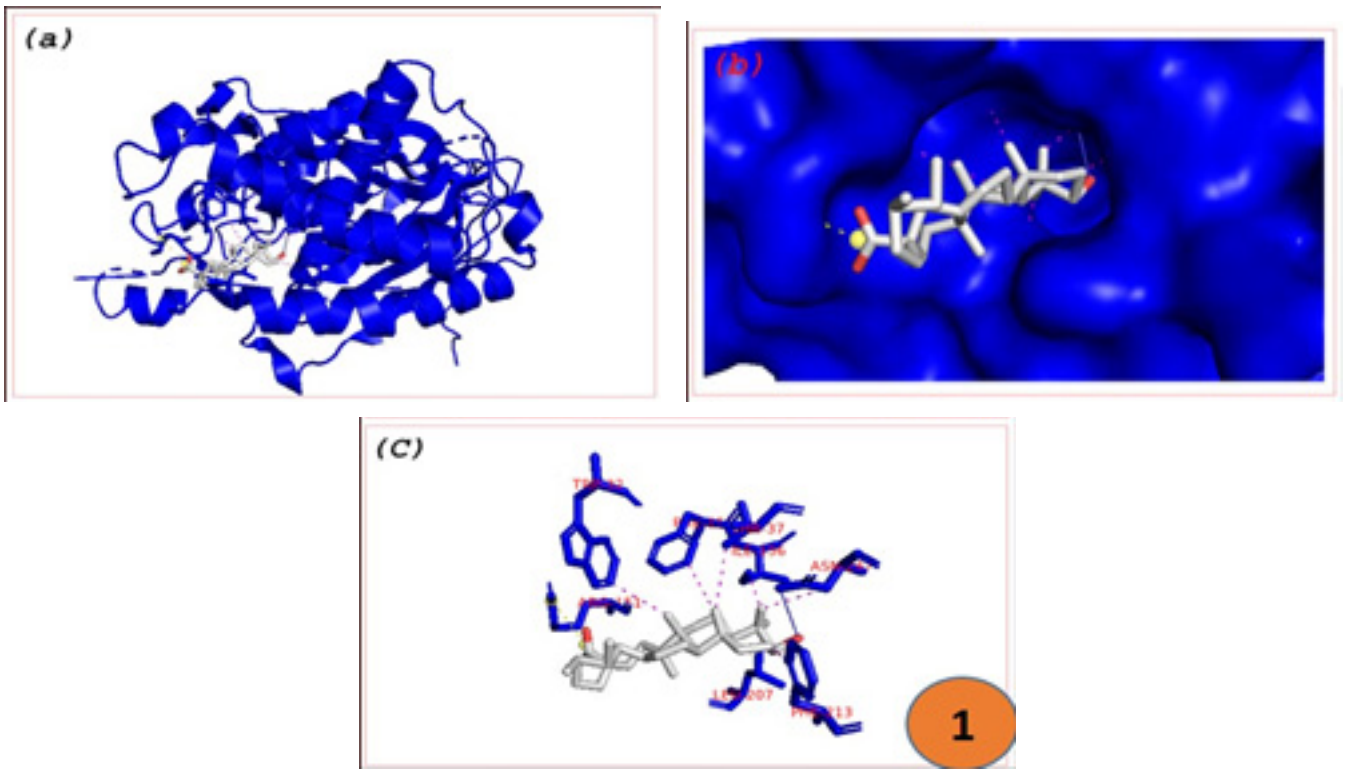

Fig. (1). Molecular interaction between FabH and L1 (**a**) complete protein with L1; (**b**) surface view; (**c**) 2D-interaction plot. (*A higher resolution / colour version of this figure is available in the electronic copy of the article*).

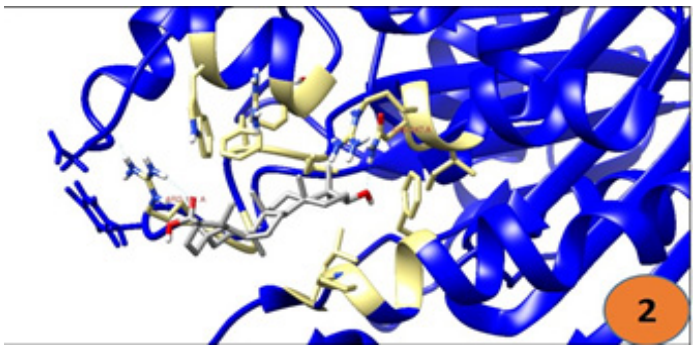

Fig. (2). Structure of FabH-L1 complex was analyzed to reflect the distribution of FabH molecules surrounding L1. (*A higher resolution / colour version of this figure is available in the electronic copy of the article*).

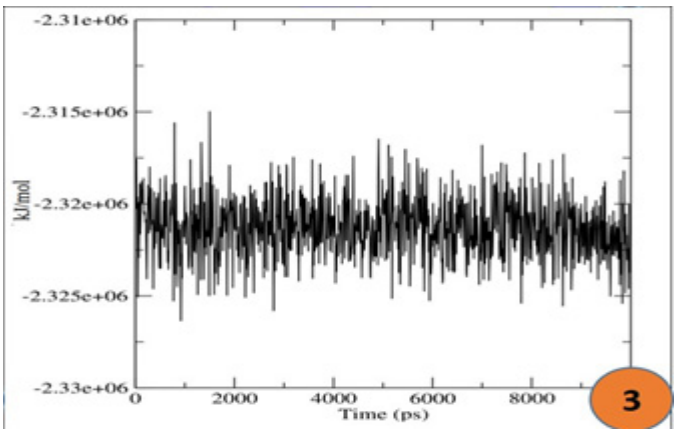

Fig. (3). MD simulation showing potential energy of protein.

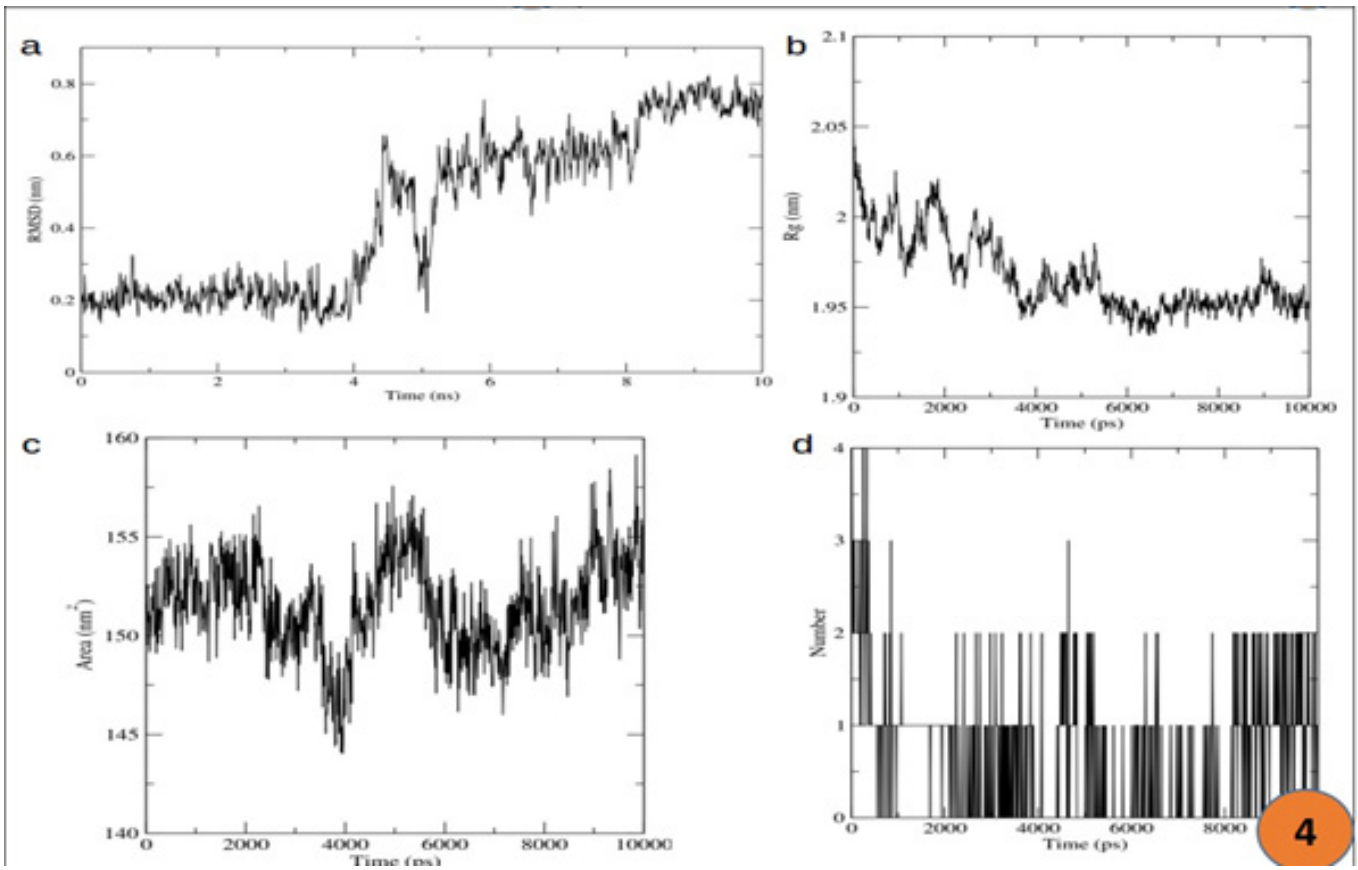

Fig. (4). MD simulation: (**a**) rmsd trajectory of protein, (**b**) radius of gyration, (**c**) SASA of protein, and (**d**) H-bond formation stability. (*A higher resolution / colour version of this figure is available in the electronic copy of the article*).

good binding with protein and was in stable conformation at the binding site.

4. DISCUSSION

In silico drug designing and molecular docking are the indispensable tools used in drug design studies. They have got tremendous attention; because of these computational approaches, the overall cost of novel drug discovery has been reduced by accelerating the efficiency in the discovery process. Mtb poses a severe danger to humans; various strains of Mtb have multiplied the issue. The disease-causing pathogen shows resistance to several drugs. Several important pathogenic enzymes play a vital role in the survival of MTB in the host environment, such as cell wall biogenesis, signal transduction, *etc.* Extensive research on TB in the last decade has discovered a list of key enzymes; most of them are absent in humans such as GlmS, GlmM, GlmU,MurA, MurB, MurC, MurD, MurE and MurF [42]. This enabled scientists to design and create drugs to fight against TB using these selective and druggable proteins as a target. However, most of these proteins cannot be targeted by all standard drugs. Thus, a mixture of drugs is being used for the therapy of TB these days. This raises the general amount of toxicity and also takes longer time to heal TB (average of six months). In this study, we selected two phytochemicals from *C. colocynthis* ursolic acid (L1) and cucurbitacin E 2-0-β-d-glucopyranoside (L2) that have been already validated to have antimycobacterial activity [22] and screened against eight potential MTB target proteins. Existing drugs were used as control to detect the binding affinity of our ligands against the target proteins.

ICL plays a crucial role in the persistence and virulence of the Mtb strain and converts isocitrate into succinate and glyoxylate. L1 showed a greater binding affinity of -8.4 kcal/mol with ICL, lower than L2 and rifampicin. Soon after the discovery of the rifampicin (1957), it is widely used against TB. Among the thirteen KI used in the study, rifampicin revealed the best binding affinity (-7.4 kcal/mol). A recent report showed that a high dosage of rifampicin is safe and well-tolerated for the whole treatment duration [38]. Interestingly, our second ligand *i.e.* L2, showed greater binding affinity (-9.7 kcal/mol) than rifampicin. L1 showed inhibition constant value of 7.05 micromolar, whereas, 50.04 by L2. L1 showed a strong hydrogen bond with ICL (contact distance 1.96 Angstrom) whereas, L2 showed a hydrogen bond distance of 2.47 Angstrom. L2 showed more hydrophobic interaction with ICL than L1.

DprE1 catalyzes epimerization reaction and helps in the production of arabinans, which is an essential component of the cell wall. Several studies have used this enzyme as a key target to design anti-TB drugs [43]. Three known inhibitors used in the present study *i.e.* rifampicin, streptomycin and kanamycin showed binding affinity score above -7.0 kcal/mol. However, both our ligands showed a better score (-9.5 kcal/mol) than the 3 known inhibitors. L1 showed inhibition constant value of 2.13 micromolar, whereas, L2 showed

5.95 micromolar for DprE1. DprE1 showed a strong hydrogen bond via. Phe231, Tyr297, Pro316 with L1 (contact distance of 2.69, 3.54, 2.42 Angstrom, respectively). As compared to L1, L2 showed a single H-bond with DprE1 *via* Tyr297 (distance: 3.64 Angstrom). Moreover, L1 carboxylate group showed salt bridge formation with Arg242 of DprE1.

Salt bridge is a strong non-covalent molecular interaction, used to design the strongest interaction in the ligand-protein complexes [44]. For the production of another important mycobacterium cell wall component, mycolic acid FabH enzyme is needed [45]. FabH initiates the synthesis of mycolic acids. Similar to DprE1, FabH also showed the same binding affinity with L1 and L2 (-9.4 kcal/mol) (Fig. **1**). L1 showed the inhibition constant value better than L2, *i.e.* 1.19 and 23.3 micromoles, respectively. L1 showed better intermolecular interactions (8 residues in hydrophobic interaction) than L2 (3 residues only). Additionally, L1 formed a salt bridge with FabH via carboxylate group of L1 and Arg151 of protein. The presence of the salt bridge further confirms the binding affinity between the protein and ligands.

Mycobactin searches for non-heme iron for Mtb. MS synthesizes mycobactin needed for Mtb survival. L2 showed binding affinity above -10.6 kcal/mol for MS, whereas, L1 showed -9.2 kcal/mol. Inhibition constants were 5.83 and 6.71 micromolar for the L1 and L2, respectively. MS with L1 and MS with L2 showed moderate intermolecular interactions (L1>L2).

RmlC plays a role in cell wall biosynthesis in Mtb. RmIC is not present in humans, thereby, it is considered as a selective target for drug discovery. Several attempts have been made to target this enzyme to produce TB treatment. Five KI namely rifampicin, streptomycin, kanamycin, ofloxacin and sparfloxacin showed binding affinity score above -7.5 kcal/mol. L1 and L2 showed lower binding affinity score than KIs *i.e.* -9.0 kcal/mol and -9.4 kcal/mol, respectively. Here again L1 showed salt bridge formation with the target protein RmIC.

NagA is involved in the first step of amino-sugar-nucleotide biosynthesis. For NagA, rifampicin showed the best binding affinity *i.e.* -9.5 kcal/mol better than L1 and L2.

ASRR showed binding affinity higher than -8.0kcal/mol. The inhibition constant values were15.14 and 321.46 micromol for L1 and L2, respectively.

Amongst all the ligands used as an i0nhibitor docked against all the proteins, CARD showed the best binding affinity score of -10.8 kcal/mol for L2. Rifampicin and L1 showed -10.8 kcal/mol and -10.1 kcal/mol, respectively for CARD. L2 showed a number of hydrogen bonds formation with CARD, revealing stronger ligand-protein complex. L1 illustrated lesser inhibition constant value *i.e.* 4.44 micromole as compared to L2 (22.76 micromole).

Analysis of intermolecular interaction enables to optimize ligand-target contacts. From the outcomes of intermolecular interaction, it becomes apparent that hydrophobic interactions play an important part in complex structural stability in all the docked structures of L1 and L2 with the target proteins. It is very interesting to note that none of the Mtb's KI has a better docking score and inhibition constant than L2. To compare L2 bonding pattern with KIs, a pharmacophore was created using LigandScout 3.0 for each ligand and compared to L2. Moreover a massive pharmacophore combining all pharmacophores of KI was also developed and pharmacophore of L2 was superimposed on it to see if L2 has the same amino acid residue bonding with that of KI. It was observed that there were some common residues that were hit by both L2 and the KI. Moreover, L2 also hit some amino acid residues that were not hit by the KI but these are the active site residues of the target as per the record of Q-site portal [46]. This demonstrates that L2 can be similar in terms of the effectiveness of eight KI aggregates.

The current study showed that Beta-Ketoacyl-Acyl Carrier Protein Synthase III (FabH) acts as a potential drug target against *M. tuberculosis* and all 15 natural compounds investigated may act as potential inhibitors for crucial target Beta-Ketoacyl-Acyl Carrier Protein Synthase III, which in turn assessed the survival of *M. tuberculosis*. Among 15 natural compounds investigated in this study, Ursolic acid (L1), which is also known for variety of biological effects such as anti-inflammation, hepatoprotection, antihyperglycemia, and antitumor promotion showed minimum binding energy with the formation of 2-4 H-bonds and also showed a fair stability within the complex in molecular dynamics studies also. Thus, ursolic acid may act as a potential lead for the additional *in vivo* studies.

CONCLUSION

Molecular docking is used to approximate a ligand's chance of binding to a protein target. In the present study, we selected two ligands ursolic acid (L1) and cucurbitacin E 2-0-β-d-glucopyranoside (L2); their docking assessment was carried out against eight target proteins. Cucurbitacin E 2-0-β-d-glucopyranoside exhibited better docking energy as compared with other known anti-TB drugs. Therefore, this research can be useful in the creation of new, multi-targeted and effective anti-TB drugs. In order to confirm their real therapeutic efficacy and drug capacity towards TB, additional in-vivo studies are required.

ETHICS APPROVAL AND CONSENT TO PARTICIPATE

Not applicable.

HUMAN AND ANIMAL RIGHTS

No animals/humans were used for studies that are base of this research.

CONSENT FOR PUBLICATION

Not applicable.

AVAILABILITY OF DATA AND MATERIALS

Not applicable.

FUNDING

None.

CONFLICT OF INTEREST

The authors declare no conflict of interest, financial or otherwise.

ACKNOWLEDGEMENTS

The authors would like to extend their sincere appreciation to the Researchers Supporting Project number **(RSP-2019/154)**, King Saud University, Riyadh, Saudi Arabia.

REFERENCES

[1] Turner, R.D.; Bothamley, G.H. Cough and the transmission of tuberculosis. *J. Infect. Dis.,* **2015**, *211*(9), 1367-1372. http://dx.doi.org/10.1093/infdis/jiu625 PMID: 25387581

[2] Muñoz, L.; Stagg, H.R.; Abubakar, I. Diagnosis and management of latent tuberculosis infection. *Cold Spring Harb. Perspect. Med.,* **2015**, *5*(11)a017830 http://dx.doi.org/10.1101/cshperspect.a017830 PMID: 26054858

[3] Cadena, J.; Rathinavelu, S.; Lopez-Alvarenga, J.C.; Restrepo, B.I. The re-emerging association between tuberculosis and diabetes: Lessons from past centuries. *Tuberculosis (Edinb.),* **2019**, *116S*, S89-S97. http://dx.doi.org/10.1016/j.tube.2019.04.015 PMID: 31085129

[4] National Academies of Sciences E. Medicine. Addressing Continuous Threats: HIV/AIDS, Tuberculosis, and Malaria.*Global Health and the Future Role of the United States*; National Academies Press: US, **2017**.

[5] Cambau, E.; Drancourt, M. Steps towards the discovery of Mycobacterium tuberculosis by Robert Koch, 1882. *Clin. Microbiol. Infect.,* **2014**, *20*(3), 196-201. http://dx.doi.org/10.1111/1469-0691.12555 PMID: 24450600

[6] Marrakchi, H.; Lanéelle, M.A.; Daffé, M. Mycolic acids: structures, biosynthesis, and beyond. *Chem. Biol.,* **2014**, *21*(1), 67-85. http://dx.doi.org/10.1016/j.chembiol.2013.11.011 PMID: 24374164

[7] Ahmed, M.M.; Velayati, A.A.; Mohammed, S.H. Epidemiology of multidrug-resistant, extensively drug resistant, and totally drug resistant tuberculosis in Middle East countries. *Int. J. Mycobacteriol.,* **2016**, *5*(3), 249-256. http://dx.doi.org/10.1016/j.ijmyco.2016.08.008 PMID: 27847005

[8] Rattan, A.; Kalia, A.; Ahmad, N. Multidrug-resistant Mycobacterium tuberculosis: molecular perspectives. *Emerg. Infect. Dis.,* **1998**, *4*(2), 195-209. http://dx.doi.org/10.3201/eid0402.980207 PMID: 9621190

[9] Shukla, R.; Shukla, H.; Sonkar, A.; Pandey, T.; Tripathi, T. Structure-based screening and molecular dynamics simulations offer novel natural compounds as potential inhibitors of Mycobacterium tuberculosis isocitrate lyase. *J. Biomol. Struct. Dyn.,* **2018**, *36*(8), 2045-2057. http://dx.doi.org/10.1080/07391102.2017.1341337 PMID: 28605994

[10] Birch, H.L. Molecular and biochemical characterisation of novel glycosyltransferases in Mycobacterium tuberculosis., Ph.D. Thesis, University of Birmingham, UK , **2011**.

[11] Veyron-Churlet, R.; Molle, V.; Taylor, R.C.; Brown, A.K.; Besra, G.S.; Zanella-Cléon, I.; Fütterer, K.; Kremer, L. The Mycobacterium tuberculosis β-ketoacyl-acyl carrier protein synthase III activity is inhibited by phosphorylation on a single threonine residue. *J. Biol. Chem.,* **2009**, *284*(10), 6414-6424. http://dx.doi.org/10.1074/jbc.M806537200 PMID: 19074144

[12] Madigan, C.A.; Martinot, A.J.; Wei, J.R.; Madduri, A.; Cheng, T.Y.; Young, D.C.; Layre, E.; Murry, J.P.; Rubin, E.J.; Moody, D.B. Lipidomic analysis links mycobactin synthase K to iron uptake and virulence in M. tuberculosis. *PLoS Pathog.,* **2015**, *11*(3)e1004792 http://dx.doi.org/10.1371/journal.ppat.1004792 PMID: 25815898

[13] Yadav, V.; Panilaitis, B.; Shi, H.; Numuta, K.; Lee, K.; Kaplan, D.L. N-acetylglucosamine 6-phosphate deacetylase (nagA) is required for N-acetyl glucosamine assimilation in Gluconacetobacter xylinus. *PLoS One,* **2011**, *6*(6)e18099 http://dx.doi.org/10.1371/journal.pone.0018099 PMID: 21655093

[14] Jensen, D.; Manzano, A.R.; Rammohan, J.; Stallings, C.L.; Galburt, E.A. CarD and RbpA modify the kinetics of initial transcription and slow promoter escape of the Mycobacterium tuberculosis RNA polymerase. *Nucleic Acids Res.,* **2019**, *47*(13), 6685-6698. http://dx.doi.org/10.1093/nar/gkz449 PMID: 31127308

[15] Mushtaq, S.; Abbasi, B.H.; Uzair, B.; Abbasi, R. Natural products as reservoirs of novel therapeutic agents. *EXCLI J.,* **2018**, *17*, 420-451. PMID: 29805348

[16] Al-Snafi, A.E. Chemical constituents and pharmacological effects of Cynodon dactylon-A review. *IOSR J. Pharm.,* **2016**, *6*(7), 17-31. http://dx.doi.org/10.9790/3013-06721731

[17] Gupta, V.K.; Kumar, M.M.; Bisht, D.; Kaushik, A. Plants in our combating strategies against Mycobacterium tuberculosis: progress made and obstacles met. *Pharm. Biol.,* **2017**, *55*(1), 1536-1544. http://dx.doi.org/10.1080/13880209.2017.1309440 PMID: 28385088

[18] Jesus, J.A.; Lago, J.H.; Laurenti, M.D.; Yamamoto, E.S.; Passero, L.F. Antimicrobial activity of oleanolic and ursolic acids: an update. *Evid. Based Complement. Alternat. Med.,* **2015**, *2015*620472 http://dx.doi.org/10.1155/2015/620472 PMID: 25793002

[19] Jyoti, M.A.; Nam, K.W.; Jang, W.S.; Kim, Y.H.; Kim, S.K.; Lee, B.E.; Song, H.Y. Antimycobacterial activity of methanolic plant extract of Artemisia capillaris containing ursolic acid and hydroquinone against Mycobacterium tuberculosis. *J. Infect. Chemother.,* **2016**, *22*(4), 200-208. http://dx.doi.org/10.1016/j.jiac.2015.11.014 PMID: 26867795

[20] López-García, S.; Castañeda-Sanchez, J.I.; Jiménez-Arellanes, A.; Domínguez-López, L.; Castro-Mussot, M.E.; Hernández-Sanchéz, J.; Luna-Herrera, J. Macrophage activation by ursolic and oleanolic acids during mycobacterial infection. *Molecules,* **2015**, *20*(8), 14348-14364. http://dx.doi.org/10.3390/molecules200814348 PMID: 26287131

[21] Podder, B.; Jang, W.S.; Nam, K.W.; Lee, B.E.; Song, H.Y. Ursolic acid activates intracellular killing effect of macrophages during Mycobacterium tuberculosis infection. *J. Microbiol. Biotechnol.,* **2015**, *25*(5), 738-744. http://dx.doi.org/10.4014/jmb.1407.07020 PMID: 25406534

[22] Mehta, A.; Srivastva, G.; Kachhwaha, S.; Sharma, M.; Kothari, S.L. Antimycobacterial activity of Citrullus colocynthis (L.) Schrad. against drug sensitive and drug resistant Mycobacterium tuberculosis and MOTT clinical isolates. *J. Ethnopharmacol.,* **2013**, *149*(1), 195-200. http://dx.doi.org/10.1016/j.jep.2013.06.022 PMID: 23816500

[23] Dushenkov, V.; Raskin, I. New strategy for the search of natural biologically active substances. Rus. *Russ. J. Plant Physiol.,* **2008**, *55*(4), 564-567. http://dx.doi.org/10.1134/S1021443708040201 PMID: 19578478

[24] Bhusal, R.P.; Bashiri, G.; Kwai, B.X.C.; Sperry, J.; Leung, I.K.H. Targeting isocitrate lyase for the treatment of latent tuberculosis. *Drug Discov. Today,* **2017**, *22*(7), 1008-1016. http://dx.doi.org/10.1016/j.drudis.2017.04.012 PMID: 28458043

[25] Manina, G.; Pasca, M.R.; Buroni, S.; De Rossi, E.; Riccardi, G. Decaprenylphosphoryl-β-D-ribose 2′-epimerase from Mycobacterium tuberculosis is a magic drug target. *Curr. Med. Chem.,* **2010**, *17*(27), 3099-3108. http://dx.doi.org/10.2174/092986710791959693 PMID: 20629622

[26] Sachdeva, S.; Reynolds, K.A. Mycobacterium tuberculosis β-Ketoacyl Acyl Carrier Protein Synthase III (mtFabH) Assay: Principles and Method.*New Antibiotic Targets*; Springer, **2008**, pp. 205-213. http://dx.doi.org/10.1007/978-1-59745-246-5_16

[27] Ma, Y.; Stern, R.J.; Scherman, M.S.; Vissa, V.D.; Yan, W.; Jones, V.C.; Zhang, F.; Franzblau, S.G.; Lewis, W.H.; McNeil, M.R. Drug targeting Mycobacterium tuberculosis cell wall synthesis: genetics of dTDP-rhamnose synthetic enzymes and development of a microtiter plate-based screen for inhibitors of conversion of dTDP-glucose to dTDP-rhamnose. *Antimicrob. Agents Chemother.,* **2001**, *45*(5), 1407-1416. http://dx.doi.org/10.1128/AAC.45.5.1407-1416.2001 PMID: 11302803

[28] Davies, J.S.; Coombes, D.; Horne, C.R.; Pearce, F.G.; Friemann, R.; North, R.A.; Dobson, R.C.J. Functional and solution structure

studies of amino sugar deacetylase and deaminase enzymes from Staphylococcus aureus. *FEBS Lett.,* **2019**, *593*(1), 52-66. http://dx.doi.org/10.1002/1873-3468.13289 PMID: 30411345

[29] Preiss, L.; Langer, J.D.; Yildiz, Ö.; Eckhardt-Strelau, L.; Guillemont, J.E.; Koul, A.; Meier, T. Structure of the mycobacterial ATP synthase Fo rotor ring in complex with the anti-TB drug bedaquiline. *Sci. Adv.,* **2015**, *1*(4)e1500106 http://dx.doi.org/10.1126/sciadv.1500106 PMID: 26601184

[30] Wawrocki, S.; Druszczynska, M. Inflammasomes in *Mycobacterium tuberculosis*-Driven Immunity. *Can. J. Infect. Dis. Med. Microbiol.,* **2017**, *2017*2309478 http://dx.doi.org/10.1155/2017/2309478 PMID: 29348763

[31] Banerjee, P.; Eckert, A.O.; Schrey, A.K.; Preissner, R. ProTox-II: a webserver for the prediction of toxicity of chemicals. *Nucleic Acids Res.,* **2018**, *46*(W1), W257-W263. http://dx.doi.org/10.1093/nar/gky318 PMID: 29718510

[32] Hanwell, M.D.; Curtis, D.E.; Lonie, D.C.; Vandermeersch, T.; Zurek, E.; Hutchison, G.R. Avogadro: an advanced semantic chemical editor, visualization, and analysis platform. *J. Cheminform.,* **2012**, *4*(1), 17. http://dx.doi.org/10.1186/1758-2946-4-17 PMID: 22889332

[33] O'Boyle, N.M.; Banck, M.; James, C.A.; Morley, C.; Vandermeersch, T.; Hutchison, G.R. Open Babel: An open chemical toolbox. *J. Cheminform.,* **2011**, *3*(1), 33. http://dx.doi.org/10.1186/1758-2946-3-33 PMID: 21982300

[34] Trott, O.; Olson, A.J. AutoDock Vina: improving the speed and accuracy of docking with a new scoring function, efficient optimization, and multithreading. *J. Comput. Chem.,* **2010**, *31*(2), 455-461. PMID: 19499576

[35] Morris, G.M.; Huey, R.; Lindstrom, W.; Sanner, M.F.; Belew, R.K.; Goodsell, D.S.; Olson, A.J. AutoDock4 and AutoDockTools4: Automated docking with selective receptor flexibility. *J. Comput. Chem.,* **2009**, *30*(16), 2785-2791. http://dx.doi.org/10.1002/jcc.21256 PMID: 19399780

[36] Hess, B.; Kutzner, C.; van der Spoel, D.; Lindahl, E. Van Der Spoel, D; Lindahl, E. GROMACS 4: algorithms for highly efficient, load-balanced, and scalable molecular simulation. *J. Chem. Theory Comput.,* **2008**, *4*(3), 435-447. http://dx.doi.org/10.1021/ct700301q PMID: 26620784

[37] Gurung, A.B.; Bhattacharjee, A.; Ali, M.A. Exploring the physicochemical profile and the binding patterns of selected novel anticancer Himalayan plant derived active compounds with macromolecular targets. *Inform. Med. Unlocked,* **2016**, *5*, 1-14. http://dx.doi.org/10.1016/j.imu.2016.09.004

[38] Seijger, C.; Hoefsloot, W.; Bergsma-de Guchteneire, I.; Te Brake, L.; van Ingen, J.; Kuipers, S.; van Crevel, R.; Aarnoutse, R.; Boeree, M.; Magis-Escurra, C. High-dose rifampicin in tuberculosis: Experiences from a Dutch tuberculosis centre. *PLoS One,* **2019**, *14*(3)e0213718 http://dx.doi.org/10.1371/journal.pone.0213718 PMID: 30870476

[39] LoBue, P.A.; Moser, K.S. Use of isoniazid for latent tuberculosis infection in a public health clinic. *Am. J. Respir. Crit. Care Med.,* **2003**, *168*(4), 443-447. http://dx.doi.org/10.1164/rccm.200303-390OC PMID: 12746255

[40] den Hertog, A.L.; Menting, S.; Pfeltz, R.; Warns, M.; Siddiqi, S.H.; Anthony, R.M. Pyrazinamide is active against Mycobacterium tuberculosis cultures at neutral pH and low temperature. *Antimicrob. Agents Chemother.,* **2016**, *60*(8), 4956-4960. http://dx.doi.org/10.1128/AAC.00654-16 PMID: 27270287

[41] Murray, J.F.; Schraufnagel, D.E.; Hopewell, P.C. Treatment of tuberculosis. A historical perspective. *Ann. Am. Thorac. Soc.,* **2015**, *12*(12), 1749-1759. http://dx.doi.org/10.1513/AnnalsATS.201509-632PS PMID: 26653188

[42] Saxena, A.K.; Singh, A. Mycobacterial tuberculosis Enzyme Targets and their Inhibitors. *Curr. Top. Med. Chem.,* **2019**, *19*(5), 337-355. http://dx.doi.org/10.2174/1568026619666190219105722 PMID: 30806318

[43] Brecik, M.; Centárová, I.; Mukherjee, R.; Kolly, G.S.; Huszár, S.; Bobovská, A.; Kilacsková, E.; Mokošová, V.; Svetlíková, Z.; Šarkan, M.; Neres, J.; Korduláková, J.; Cole, S.T.; Mikušová, K. DprE1 is a vulnerable tuberculosis drug target due to its cell wall localization. *ACS Chem. Biol.,* **2015**, *10*(7), 1631-1636. http://dx.doi.org/10.1021/acschembio.5b00237 PMID: 25906160

[44] Kurczab, R.; Śliwa, P.; Rataj, K.; Kafel, R.; Bojarski, A.J. Salt bridge in ligand–protein complexes—systematic theoretical and statistical investigations. *J. Chem. Inf. Model.,* **2018**, *58*(11), 2224-2238. http://dx.doi.org/10.1021/acs.jcim.8b00266 PMID: 30351056

[45] Scarsdale, J.N.; Kazanina, G.; He, X.; Reynolds, K.A.; Wright, H.T. Crystal structure of the Mycobacterium tuberculosis beta-ketoacyl-acyl carrier protein synthase III. *J. Biol. Chem.,* **2001**, *276*(23), 20516-20522. http://dx.doi.org/10.1074/jbc.M010762200 PMID: 11278743

[46] Laurie, A.T.; Jackson, R.M. Q-SiteFinder: an energy-based method for the prediction of protein-ligand binding sites. *Bioinformatics,* **2005**, *21*(9), 1908-1916. http://dx.doi.org/10.1093/bioinformatics/bti315 PMID: 15701681